gridded maps of biomass to be produced over time[6].

Radar backscatter is sensitive to vegetation fresh biomass[7]. At long wavelengths (0.7 m or longer), radar penetrates deep into the canopy and the backscatter energy depends on a combination of variables including the size, number density, and the water content and wood specific gravity of branches and stems. However, radar backscatter suffers from gradual loss of sensitivity as biomass increases. The phenomenon referred to as 'saturation' occurs often in radar backscatter at shorter wavelengths, but is not unique to radar and forests, and can occur in all types of remote-sensing measurements, even for non-woody vegetation. However, at longer wavelengths (>0.7 m), radar backscatter remains sensitive to a wide range of AGB.

Variation in tree density may impact radar backscatter, but does not cause loss of sensitivity. In spatially heterogeneous forests, the largest source of error in deriving the relationship between radar backscatter and biomass is from the geometry of measurement and the difference between the biomass sensed by radar and that sampled on the ground. The ground data are too often based on small inventory plots, leading to large errors that are often ignored. By increasing the plot size used for remote-sensing calibration, the relationship improves significantly[5].

Woodhouse *et al.*[1] criticize the use of regression models that convert the backscatter into AGB, which are derived using collections of sites spanning a range of forest types. Mixing data across forest types to sample a wider range of AGB is a common statistical approach used not only in most remote-sensing studies but also repeatedly in field estimation, where inventory data from a limited number of trees is used to predict AGB values over the full range of trees from different regions. Regardless of the type of models used, prediction never implies accuracy.

A systematic radar observation at long wavelengths from space, as recommended by European Space Agency's BIOMASS mission, accompanied by remote-sensing-specific field inventory data provides the only way to circumvent the limitations of field inventory-only biomass monitoring at the global scale. Extending current studies beyond the landscape scale is a priority if radar remote sensing is to fulfil its potential in the context of the Reducing Emissions from Deforestation and Forest Degradation programme (www.un-redd.org). ❐

References
1. Woodhouse, I., Mitchard, E. T. A., Brolly, M., Maniatis, D. & Ryan, C. M. *Nature Clim. Change* **2,** 556–557 (2012).
2. Clark, D. & Kellner, J. *J. Veg. Sci.* **23,** 1191–1196 (2012).
3. Chave, J. *et al. Phil. Trans. R. Soc. B* **359,** 409–420 (2004).
4. Saatchi, S. *et al. Proc. Natl Acad. Sci. USA* **108,** 9899–9904 (2011).
5. Sandberg, G. *et al. Remote Sens. Environ.* **115,** 2874–2886 (2011).
6. Shugart, H., Saatchi, S. & Hall, F. *J. Geophys. Res.* **115,** G00E03 (2010).
7. LeToan, C. *et al. IEEE Trans. Geosci. Remote* **30,** 403–411 (1992).

Sassan Saatchi[1]*, Lars Ulander[2], Mathew Williams[3], Shaun Quegan[4], Thuy LeToan[5], Herman Shugart[6] and Jerome Chave[7]
[1]Jet Propulsion Laboratory, California Institute of Technology, Pasadena, California 91109, USA, [2]Department of Earth and Space Science, Chalmers University of Technology, 412 96 Göteborg, Sweden, [3]University of Edinburgh, Drummond Street, Edinburgh EH8 9XP, UK, [4]Centre for Terrestrial Carbon Dynamics, University of Sheffield, Sheffield S3 7RH, UK, [5]Centre d'Etudes Spatiales de la Biosphère, 31401 Toulouse, France, [6]University of Virginia, Charlottesville, Virginia 22904, USA, [7]CNRS, Université Paul Sabatier, UMR 5174, Toulouse, France.
*e-mail: Saatchi@jpl.nasa.gov

CORRESPONDENCE:

Drought-induced decline in Mediterranean truffle harvest

To the Editor — With a price of up to €2,000 kg^{-1} the Périgord black truffle (*Tuber melanosporum*; hereinafter truffle) is one of the most exclusive delicacies[1]. However, harvests of this ectomycorrhizal ascomycete have declined in its natural Mediterranean habitat[2], despite cultivation efforts since the 1970s[3]. Satisfying explanations for the long-term decrease in both natural and planted truffle yields are lacking. Understanding microbial below-ground processes remains challenging because experimental settings generally don't have the necessary degree of real-world complexity[4], long enough mycological observations are scarce[5] and quantitative information from natural truffle habitats and plantations is usually not available[2,3,6].

Here we seek to understand how climate can affect truffle production, either directly, or indirectly via their symbiotic host plants. We did this by analysing annual inventories of regional truffle harvests from northeastern Spain (Aragón), southern France (Périgord), and northern Italy (Piedmont and Umbria) (Supplementary Fig. S1 and Table S1). We found that changes in truffle production (tons yr^{-1} from 1970–2006) were most similar between Aragón and Périgord ($r = 0.59$; $p < 0.001$), and non-significant between Périgord and Piedmont–Umbria ($r = 0.12$). The observed regional-scale coherency probably originates from common climatic cues that synchronize truffle fruiting among large parts of the western Mediterranean Basin. Spanish and French truffle harvests showed significant positive correlation with summer rainfall ($r = 0.72$ and 0.43; $p < 0.001$), whereas lower agreement was found between Italian truffle production and precipitation ($r = 0.22$; Supplementary Fig. S2). These different sensitivity levels seem reasonable as the Italian truffières are generally experiencing twice as much summer rainfall as the Spanish areas, with the French sites ranging in between (Supplementary Fig. S3).

When averaging the three truffle records (Supplementary Table S1), their subcontinental mean correlates positively and negatively at the 99.9% significance level with gridded June–August precipitation totals and temperature maxima ($r = 0.60$ and -0.57), respectively (Fig. 1a,b). Natural and cultivated Mediterranean truffle yields — seasonally restricted to November–February[3] — depend on variations in summer climate[6], with wet and cold conditions promoting fruit body formation. Given the symbiotic fungi–host association[7], we postulate that competition for summer soil moisture between host plants and their mycorrhizal

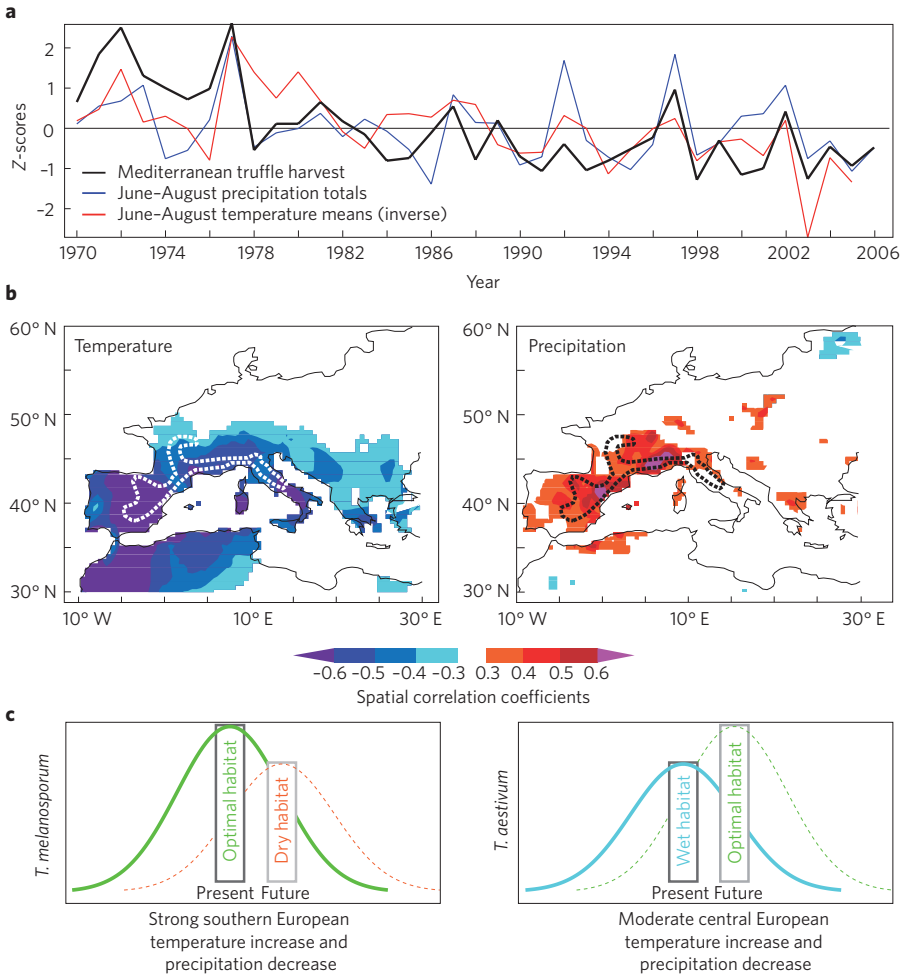

Figure 1 | Truffle yield and climate change. **a**, Comparison of Mediterranean truffle harvests (tons yr^{-1}) and variations in June–August temperature means (inverse) and precipitation totals averaged over 35–50° N and 10° W–20° E (see Supplementary Information for details). All time series were normalized to have means of 0 and standard deviations of 1 over their common period 1970–2006. Annual truffle harvest correlates at the 99.9% significance level with inverse temperature means ($r = 0.59$) and precipitation totals ($r = 0.60$) over 1970–2006. First-order autocorrelation (*lag-1*) of the truffle, precipitation and temperature time-series is $r = 0.48$, $r = -0.05$ and $r = 0.33$, respectively. **b**, Corresponding spatial field correlations (1970–2006) of the Mediterranean truffle record and gridded (0.5° x 0.5°) European summer (June–August) temperature means and precipitation totals (over 30–60° N and 10° W–30° E). Dashed contours indicate the natural distribution of *T. melanosporum*. **c**, A schematic overview of the observed and expected southern European *T. melanosporum* and central European *T. aestivum* fruit body (ascocarp) productions (left and right). The diagram indicates a shift from presently optimal Mediterranean growth conditions for *T. melanosporum* toward less productivity in a drier future. In contrast, *T. aestivum* growth is likely to benefit from a slightly warmer and drier climate north of the Alpine arc.

partners might be a critical factor for truffle fruit body production, particularly in semi-arid environments.

The observed response delay emphasizes complex mechanisms of carbohydrate allocation from the host plants to their fungal symbionts[6,8]. An adequate carbohydrate flux from the host tree to its roots during the vegetation period might stimulate soil mycelium growth and fruit body initialization, which is likely a prerequisite for rich winter truffle harvests. An additional carbon source for fungi fruit body production might derive from those carbohydrates that were allocated in the host trees' stem and roots during the warmer vegetation period[9]. In fact, Spanish tree growth (that is, oak ring width; Supplementary Table S2), which mainly occurs from May–July and depends on the amount of precipitation during this period (Supplementary Fig. S4), correlated positively at the 99.9% significance level ($r = 0.62$; 1970–2006) with truffle yield (Supplementary Fig. S5). This relationship implies ring width variations are a reasonable proxy for truffle fruit body production.

A suite of 12 climate models projects increasing mean temperatures and decreasing precipitation totals for the Mediterranean Basin until the end of the twenty-first century[10] (Supplementary Figs S6,S7), which subsequently denotes intensified potential summer evapotranspiration. The simulated climate envelope for southwest Europe for the past decades matched the observed decline in Mediterranean truffle harvest. It remains unclear if plant physiological and biogeochemical processes relevant for truffle fruit body formation and maturation will behave in a state-dependent, nonlinear way or if critical thresholds — so-called tipping points — at which a system shifts abruptly from one state to another will be reached under projected climate change[11]. Nevertheless, we assume that the Mediterranean truffle yield will continue to decline in response to amplified summer dryness (Fig. 1c), and we believe that calcareous regions north of the Alpine arc will possibly transform into more suitable habitats[12,13].

Spatial and seasonal alterations in future precipitation regimes and associated summer aridity will be important for the adaptation and evolution of *T. melanosporum* across its native distribution range, perhaps favouring drought-resistant strains[3]. An expected decline in Mediterranean truffle harvests — impacting rural tourism, regional agriculture and global prices[2,14] — may also enhance the value of other species that are more plastic in their metabolism and less deterministic in their ecological niche requirements[3,6]. *T. aestivum* cultivation in more temperate environments north of the Alps (Fig. 1c), as well as market demand for supplies from non-traditional Périgord black-truffle-producing countries outside Europe, will probably increase. ❐

References
1. Martin, F. *et al. Nature* **464,** 1033–1038 (2010).
2. Hall, I. R., Yun, W. & Amicucci, A. *Trends Biotech.* **21,** 433–438 (2003).
3. Mello, A., Murat, C. & Bonfante, P. *FEMS Microbiol. Lett.* **260,** 1–8 (2006).
4. Talbot, J. M., Allison, S. D. & Treseder, K. K. *Func. Ecol.* **22,** 955–963 (2008).
5. Büntgen, U., Kauserud, H. & Egli, S. *Front. Ecol. Environ.* **10,** 14–19 (2012).
6. Gallot, G. *La truffe, la terre, la vie* (INRA, 1999).

7. Lilleskov, E. A., Bruns, T. D., Dawson, T. E. & Camacho, F. J. *New Phytol.* **182,** 483–494 (2009).
8. Högberg, P. & Read, D. J. *Trends Ecol. Evol.* **21,** 548–554 (2006).
9. Waring, R. H. *BioScience* **37,** 569–574 (1987).
10. Fischer, E. M. & Schär, C. *Nature Geosci.* **3,** 398–403 (2010).
11. Scheffer, M. *et al. Nature* **461,** 53–59 (2009).
12. Büntgen, U. *et al. Front. Ecol. Environ.* **9,** 150–151 (2011).
13. Stobbe, U. *et al. Fungal Ecol.* **5,** 591–599 (2012).
14. Samils, *et al. Econ. Bot.* **62,** 331–340 (2008).

Acknowledgements
We thank I.R. Hall and F. Martínez Peña for discussions. Supported by the WSL-internal DITREC project, the Eva Mayr-Stihl Foundation, and the Czech project 'Building up a multidisciplinary scientific team focused on drought' (No. CZ.1.07/2.3.00/20.0248).

Author contributions
U.B. designed the study with input from W.T., U.S., L.S. and S.E. Analyses were performed by U.B. with support of J.J.C. and E.M.F. All authors contributed to discussion, interpretation and writing.

Additional information
Supplementary information is available in the online version of this paper. Reprints and permissions information is available online at www.nature.com/reprints. Correspondence should be addressed to U.B.

Competing financial interests
The authors declare no competing financial interests.

Ulf Büntgen[1,2,3]*, Simon Egli[1], J. Julio Camarero[4], Erich M. Fischer[5], Ulrich Stobbe[6], Håvard Kauserud[7], Willy Tegel[8], Ludger Sproll[6] and Nils C. Stenseth[9]
[1]Swiss Federal Research Institute WSL, Zucherstrasse 111, 8903 Birmensdorf, Switzerland, [2]Oeschger Centre for Climate Change Research, University of Bern, Zähringerstrasse 25, 3012 Bern, Switzerland, [3]Global Change Research Centre AS CR, v.v.i., Bělidla 986/4a, 60300 Brno, Czech Republic, [4]ARAID-Instituto Pirenaico de Ecología CSIC, Avenida Montañana 1005, 50080 Zaragoza, Spain, [5]Institute for Atmospheric and Climate Science, ETH Zürich, Universitätstrasse 16, 8092 Zürich, Switzerland, [6]Institute of Forest Botany and Tree Physiology, University of Freiburg, Bertoldsstraße 17, 79085 Freiburg, Germany, [7]Microbial Evolution Research Group, Department of Biology, University of Oslo, Postboks 1066 Blindern, 0316 Oslo, Norway, [8]Institute for Forest Growth, University of Freiburg, Tennebacher Straße 4, 79085 Freiburg, Germany, [9]Centre for Ecological and Evolutionary Synthesis CEES, Department of Biology, University of Oslo, Postboks 1066 Blindern, 0316 Oslo, Norway.
*e-mail: buentgen@wsl.ch

CORRESPONDENCE:

Arctic contaminants and climate change

To the Editor — In a recent Letter[1], Ma *et al.* analysed eight persistent organic pollutants (POPs) at an Arctic monitoring station (Mount Zeppelin, 474 metres above sea level, Svalbard). They identified inclines in the latter parts of the linearly detrended concentration time-series (1993–2009). Their interpretation is that many POPs (besides the more volatile polychlorinated biphenyls and hexachlorobenzene) have become remobilized from Arctic repositories into the atmosphere as a consequence of climate change. However, it should be emphasized that other factors can cause the reported inclines, which reflect nonlinearities (or a degree of curvature) within the data.

The eight POPs (α-HCH, γ-HCH, *cis*-NO, *trans*-CD, *o*,*p*′-DDE, *p*,*p*′-DDE, *o*,*p*′-DDT, *p*,*p*′-DDT) analyzed by Ma *et al.* exhibit declining Arctic trends due to reductions in global emissions, modified by processes such as environmental degradation and interchange between atmosphere and surface media. Ma *et al.* used a linear model to detrend the data. Notably, statistical significance of the linear fit does not preclude presence of nonlinearities within the data (indeed such nonlinearities are what lead to the reported inclines), nor does it provide information on the origins of this nonlinearity. Factors other than climate change may also cause nonlinearity or curvature in POP decline. Incline features on linear detrending can result from nonlinear decline of global emissions, nonlinearity that occurs naturally as concentrations decay towards zero or from concentrations declining to levels at which surface-to-air exchange (revolatilization) from legacy POP repositories increasingly occurs as a response to disequilibrium[2,3] (even in the absence of climate change), acting as a buffer and decelerating their declines.

Ma and colleagues' perturbation modelling predicts how enhanced revolatilization induced by climate change acts to relatively enhance Arctic POPs' atmospheric levels, as previously postulated[2,4,5]. The modelled inclines showed correlations to the incline features in the detrended data, but comparison in terms of magnitudes was limited, and some discrepancies exist. For example, interannual variability for the eight POPs appears to co-vary in the model[1] (see ref. 1, Supplementary Fig. S3) but not in the detrended measurements (data visualization; J. Ma, personal communication).

With the data available at present it is very difficult to establish quantitatively which factors (revolatilization induced by climate change, or other factors as outlined above) contribute most to nonlinearity in these eight POPs' declining trends at Mount Zeppelin. Thus, the potential for multiple sources of nonlinearity is emphasized as an important caveat to the reported identification of an observable and widespread warming-induced signature. Full visualization of the summer data analysis behind the statistics (noting differences to Fig. 1[1]) would aid readers' interpretation. ❐

References
1. Ma, J., Hung, H., Tian, C. & Kallenborn, R. *Nature Clim. Change* **1,** 255–260 (2011).
2. Nizzetto, L. *et al. Environ. Sci. Technol.* **44,** 6526–6531 (2010).
3. Dachs, J. *Nature Clim. Change*, **1,** 247–248 (2011).
4. Macdonald, R. W., Harner, T. & Fyfe, J. *Sci. Total Environ.* **342,** 5–86 (2005).
5. Lamon, L. *et al. Environ. Sci. Technol.* **43,** 5818–5824 (2009).

Acknowledgements
I am grateful to W. Tych for useful discussions on an earlier draft.

Tjarda J. Roberts
LPC2E, UMR 7328, CNRS-Université d'Orléans, 3A Avenue de la Recherche Scientifique, 45071 Orléans, Cedex 2, France.
e-mail: tjardaroberts@gmail.com

Ma *et al.* reply — Roberts[1] argues that our linear detrending analysis for the air concentration time-series of persistent organic pollutants (POPs) collected from the Mount Zeppelin Arctic monitoring site may not address nonlinearities within the air concentration data, though the time series of POPs data analysed in our study[2] exhibited statistically significant linear trends.

However, one cannot assume that the overall impact of a combination

Supplementary Information

CORRESPONDENCE: Drought-induced decline in Mediterranean truffle harvest

by U. Büntgen et al.

All correlations used in this manuscript are Pearson's Product-moment correlation coefficients. Inter-series correlations, abbreviated with the term *Rbar*, refer to grand average correlations between each time-series that was available. Significance levels were corrected for first-order autocorrelation in each time-series (i.e. we adapted the degrees of freedom in autocorrelated data).

Information on annual truffle harvest from Spain and France was compiled by the national Truffle Grower Associations and published through the head organization Groupement European Tuber GET, whereas data from Italy were collected and published by the National Institute for Statistics ISTAT.

For Spain see: La Federacion española de asociaciones de truficultores (FETT), Reyna, S., De Miguel, A., Palanzón, C., Hernández, A. 2005. Spanish trufficulture. In: Proceedings of the Fourth International Workshop on Edible Mycorrhizal Mushrooms. Murcia, Spain, 28 November–2 December 2005. Universidad de Murcia, Murcia. P. 109.

For France see: La Fédération française des trufficulteurs (FFT), Courvoisier, M. (1995) La production et les cours de la truffe d'hiver 1903–1995. Le Trufficulteur Francais 10, 8–9 and Courvoisier, M. (1995) La production et les cours de la truffe d'hiver 1903–1995. Le Trufficulteur Francais 13, 10–11.

For Italy see: La Federazione Nazionale Associazioni Tartufai Tartuficoltori (FNAT), Data collected by The National Institute for Statistics ISTAT (1961-2003) and compiled in the COST action E30 report: Pettenella, D., Klöhn, S., Brun, F., Carbone, F., Venzi, L., Cesaro, L., Ciccarese, L. 2004. Economic integration of urban consumers' demand and rural forestry production. Italy's Country Report, COST Action E30. Pp.29-38.

For details on *Quercus ilex* growth in a nearby site see: Montserrat-Marti, G. et al. (2009): Summer-drought constrains the phenology and growth of two coexisting Mediterranean oaks with contrasting leaf habit: implications for their persistence and reproduction. Trees 23: 787-799.

Table S1 | Regional truffle harvest data (tones/year) as utilized in figure S1 and S1 and the main text (Fig. 1).

Year	Spain	France	Italy	Spain & France	Spain & Italy	France & Italy	All	Spain z-scores	France z-scores	Italy z-scores	Spain & France z-scores	Spain & Italy z-scores	France & Italy z-scores	All z-scores
1970	40	40	30	80	70	70	110	0.443	0.4111	0.814	0.4775	0.6803	0.7219	0.65303174
1971	60	100	5	160	65	105	165	1.4158	2.9116	-1.031	2.4907	0.5114	1.9312	1.85025661
1972	60	100	35	160	95	135	195	1.4158	2.9116	1.183	2.4907	1.5251	2.9678	2.50328835
1973	70	40	30	110	100	70	140	1.9022	0.4111	0.814	1.2325	1.694	0.7219	1.30606349
1974	60	36	30	96	90	66	126	1.4158	0.2444	0.814	0.8801	1.3561	0.5837	1.00131534
1975	40	38	35	78	75	73	113	0.443	0.3278	1.183	0.4271	0.8493	0.8255	0.71833492
1976	50	25	50	75	100	75	125	0.9294	-0.214	2.2903	0.3516	1.694	0.8946	0.97954762
1977	70	100	30	170	100	130	200	1.9022	2.9116	0.814	2.7424	1.694	2.795	2.61212697
1978	15	15	25	30	40	40	55	-0.773	-0.631	0.4449	-0.781	-0.333	-0.315	-0.5441931
1979	40	20	25	60	65	45	85	0.443	-0.422	0.4449	-0.026	0.5114	-0.142	0.10883862
1980	30	45	10	75	40	55	85	-0.043	0.6195	-0.662	0.3516	-0.333	0.2036	0.10883862
1981	40	20	50	60	90	70	110	0.443	-0.422	2.2903	-0.026	1.3561	0.7219	0.65303174
1982	40	33	15	73	55	48	88	0.443	0.1194	-0.293	0.3013	0.1735	-0.038	0.1741418
1983	30	13	30	43	60	43	73	-0.043	-0.714	0.814	-0.454	0.3425	-0.211	-0.1523741
1984	12	11	20	23	32	31	43	-0.919	-0.797	0.0758	-0.957	-0.604	-0.626	-0.8054058
1985	5	26	15	31	20	41	46	-1.259	-0.172	-0.293	-0.756	-1.009	-0.28	-0.7401026
1986	20	20	35	40	55	55	75	-0.53	-0.422	1.183	-0.529	0.1735	0.2036	-0.1088386
1987	30	60	15	90	45	75	105	-0.043	1.2446	-0.293	0.7291	-0.164	0.8946	0.54419312
1988	8	30	6	38	14	36	44	-1.113	-0.006	-0.958	-0.579	-1.212	-0.453	-0.7836381
1989	45	14	30	59	75	44	89	0.6862	-0.672	0.814	-0.051	0.8493	-0.176	0.19590952
1990	30	17	1	47	31	18	48	-0.043	-0.547	-1.327	-0.353	-0.637	-1.075	-0.6965672
1991	10	20	1	30	11	21	31	-1.016	-0.422	-1.327	-0.781	-1.313	-0.971	-1.0666185
1992	30	31	1	61	31	32	62	-0.043	0.036	-1.327	-7E-04	-0.637	-0.591	-0.391819
1993	8	22	2	30	10	24	32	-1.113	-0.339	-1.253	-0.781	-1.347	-0.868	-1.0448508
1994	4	9	30	13	34	39	43	-1.308	-0.881	0.814	-1.209	-0.536	-0.349	-0.8054058
1995	20	11	25	31	45	36	56	-0.53	-0.797	0.4449	-0.756	-0.164	-0.453	-0.5224254
1996	25	24	20	49	45	44	69	-0.287	-0.256	0.0758	-0.303	-0.164	-0.176	-0.239445
1997	80	20	24	100	104	44	124	2.3885	-0.422	0.3711	0.9808	1.8292	-0.176	0.95777989
1998	7	10	4	17	11	14	21	-1.162	-0.839	-1.105	-1.108	-1.313	-1.213	-1.2842958
1999	35	21	10	56	45	31	66	0.1998	-0.381	-0.662	-0.127	-0.164	-0.626	-0.3047481
2000	6	17	4	23	10	21	27	-1.211	-0.547	-1.105	-0.957	-1.347	-0.971	-1.1536894
2001	20	9	5	29	25	14	34	-0.53	-0.881	-1.031	-0.806	-0.84	-1.213	-1.0013153
2002	40	39	20	79	60	59	99	0.443	0.3694	0.0758	0.4523	0.3425	0.3418	0.41358677
2003	7	9	6	16	13	15	22	-1.162	-0.881	-0.958	-1.133	-1.246	-1.179	-1.262528
2004	22	27	10	49	32	37	59	-0.432	-0.131	-0.662	-0.303	-0.604	-0.418	-0.4571222
2005	14	15	8	29	22	23	37	-0.822	-0.631	-0.81	-0.806	-0.942	-0.902	-0.9360122
2006	20	28	10	48	30	38	58	-0.53	-0.089	-0.662	-0.328	-0.671	-0.384	-0.4788899

Table S2 | Regional tree growth data as utilized in figure S4 and S5. The term *Year* refers to the absolutely dated calendar year A.D. The term *Series* refers to the number of samples that are available during this year. The abbreviation *TRW* refers to the raw tree-ring width values (mm/yr).

Year	Series	TRW	Year	Series	TRW	Year	Series	TRW	Year	Series	TRW
1970	10	1.131	1980	20	0.754	1990	20	0.953	2000	19	0.61
1971	10	2.763	1981	20	0.433	1991	20	0.714	2001	19	0.753
1972	10	2.544	1982	20	0.67	1992	20	0.456	2002	18	0.487
1973	10	2.505	1983	20	0.589	1993	20	0.582	2003	17	0.517
1974	11	1.179	1984	20	1.494	1994	20	0.516	2004	15	0.831
1975	11	0.647	1985	20	0.742	1995	20	0.436	2005	15	0.472
1976	16	0.644	1986	20	0.439	1996	20	1.001	2006	14	0.52
1977	19	1.193	1987	20	0.48	1997	20	3.218	2007	4	0.42
1978	20	0.886	1988	20	1.841	1998	19	0.687			
1979	20	1.086	1989	20	0.591	1999	19	0.975			

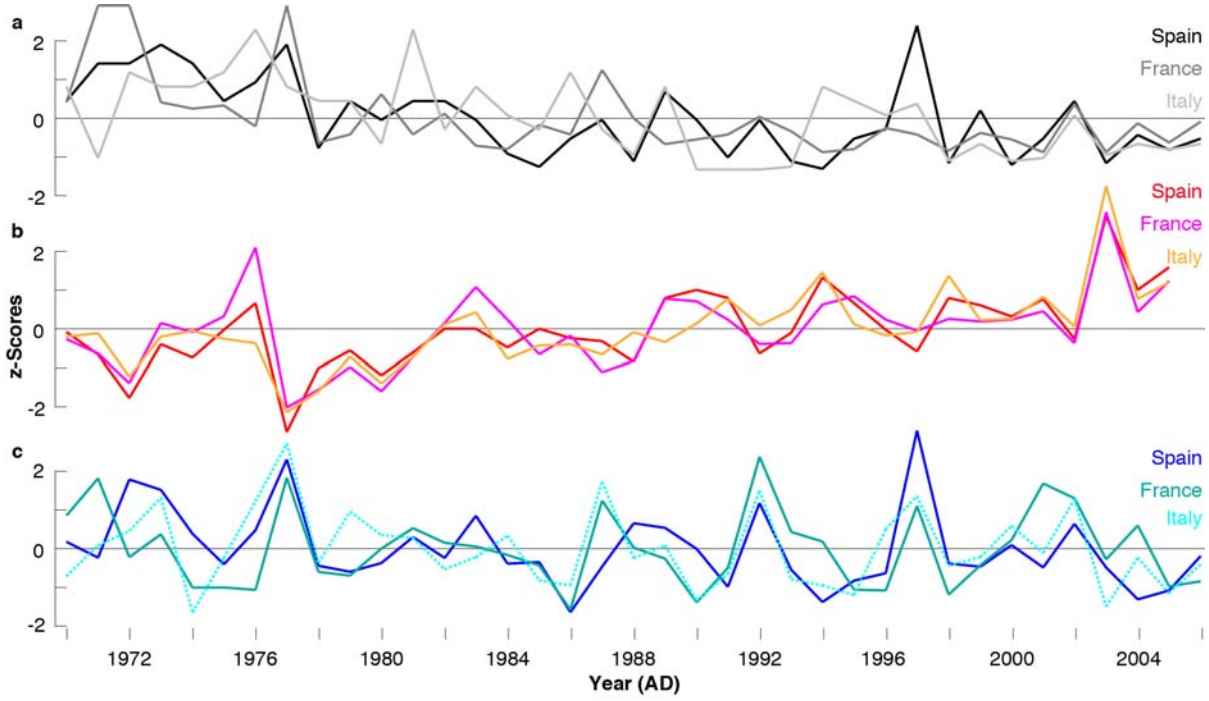

Figure S1 | Truffle harvest and climate change. **a**, Regional-scale truffle production with an inter-series correlation (*Rbar;* each series is correlated against each series) of 0.40 compared to variation in summer (June-August), **b**, temperature maxima (*Rbar* of 0.84), and **c**, precipitation totals (*Rbar* of 0.40). The individual time-series (tons/year) were normalized (mean of 0.0 and standard deviation of 1.0) over the common period 1970-2006.

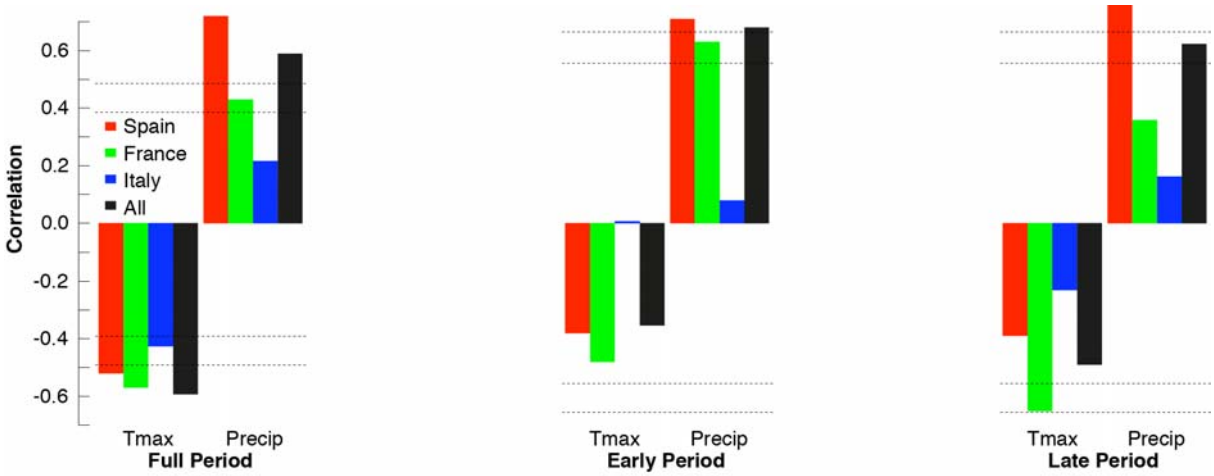

Figure S2 | Truffle harvest and climate forcing. Relationship between regional (Spanish, French and Italian) and averaged (Mediterranean) rates of truffle production and variations in summer (June-August) climate (temperature maxima and precipitation totals) computed over the full (1970-2006), early (1970-1987) and late (1988-2006) periods. Lower and upper dashed lines refer to 99.0% and 99.9% significance levels, respectively.

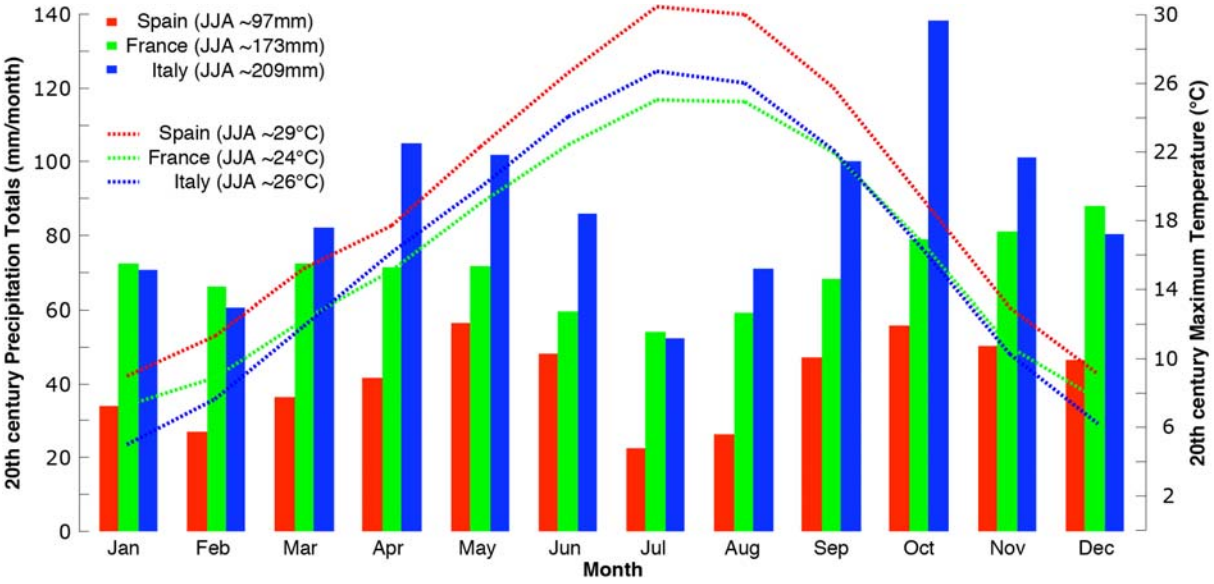

Figure S3 | Climatic background. Annual cycle of precipitation totals and temperature maxima computed for each month and the three regions in Spain (1.0-0.5°W and 41.0-41.5°N), France (0.5-1.0°E and 45.5-46.0°N) and Italy (8.0-8.5°E and 44.5-45.0°N) over the 1901-2000 period. Precipitation totals (mm) and temperature means (°C) are indicated for the June-August (JJA) summer season. Data were extracted from the gridded CRU TS 3.1 compilation via the KNMI climate explorer (http://climexp.knmi.nl).

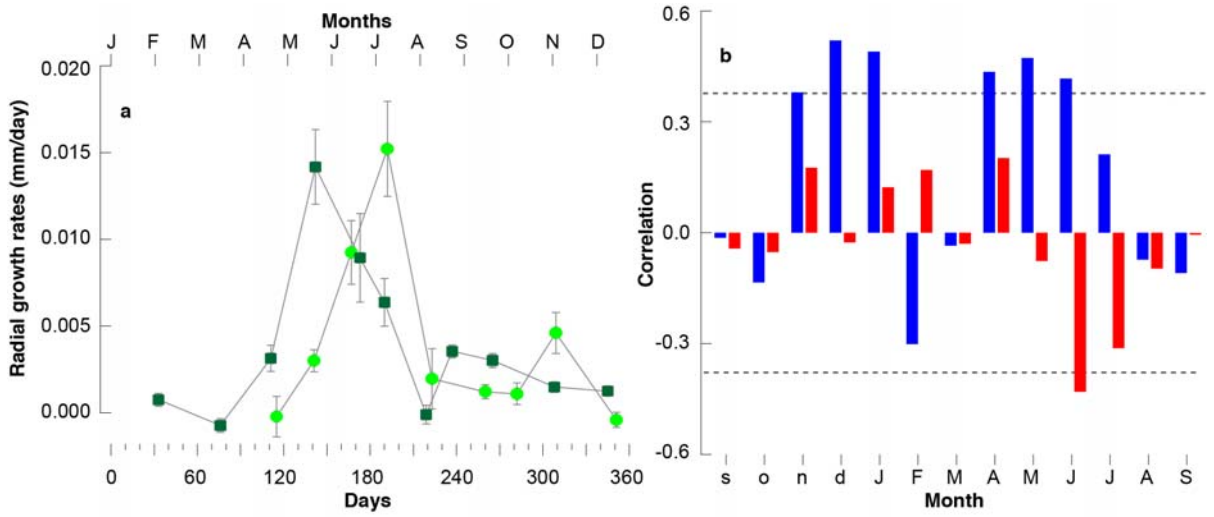

Figure S4 | Tree growth and climate. **a**, Intra-annual growth variations of radial stem increment (± SE, *n* =10 trees) obtained from manual dendrometer bands (Agriculture Electronics Corporation, Tucson, USA) in Alcubierre between 2008 and 2009 (green circles and dark-green squares). Radial growth rates (mm/day) were calculated by subtracting consecutive readings of cumulative growth rates and dividing them by the number of days elapsed between successive readings. **b**, Correlation analysis between ring width indices and monthly mean temperatures (red) and precipitation totals (blue) computed over the 1970-2007 period and using the interval from previous to current year September.

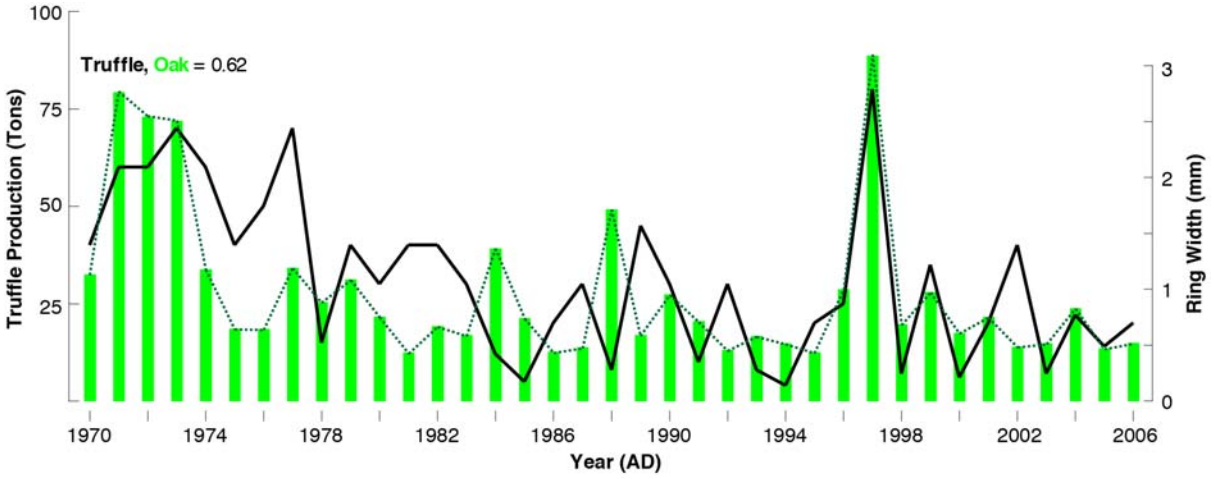

Figure S5 | Truffle harvest and tree growth. Comparison between Spanish truffle production and variation on ring width of 20 samples from eleven oak (*Quercus ilex*) trees from a site in northeast Spain (Huesca, Alcubierre, 42°18'N, 0°47'W). The annually cross-dated and well-replicated chronology covers the 1970-2006 period. Inter-series (*Rbar*) correlation in 0.82, and mean ring width is 0.95 mm.

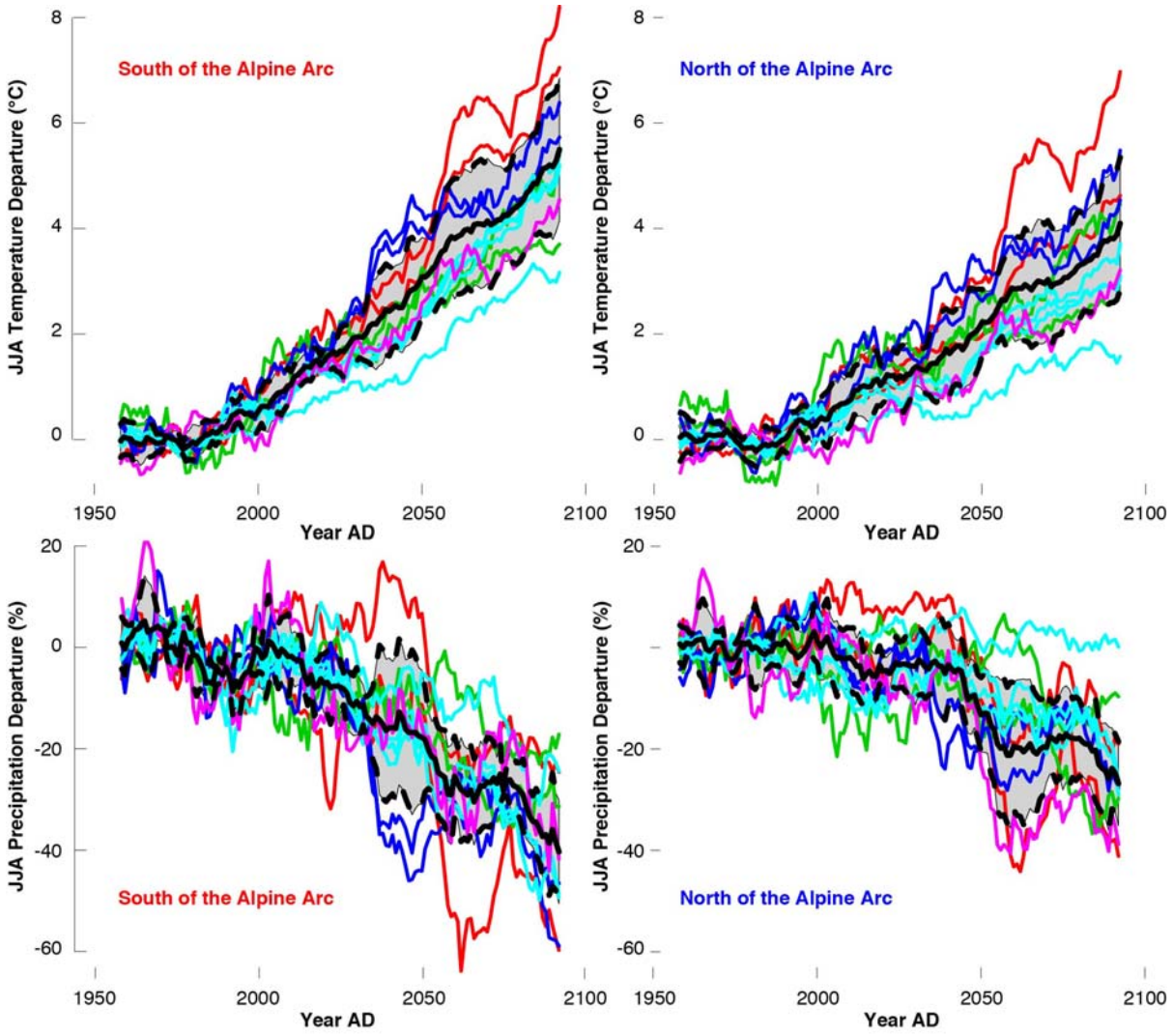

Figure S6 | Climate variations. Simulated (color lines) mean June-August (JJA) summer temperature (upper panels) and precipitation (lower panels) change (in °C and %) separated between Europe south (left) and north (right) of the Alpine arc between 1950 and 2099 AD, and expressed as 15-year moving averages with respect to 1960-1989. The simulations were performed with 12 RCMs driven with 6 GCMs forced with the SRES A1B emission scenario within the European multi-model experiment ENSEMBLES (Linden & Mitchell 2009: ENSEMBLES: Climate Change and its Impacts: Summary of research and results from the ENSEMBLES project). The solid black line indicates the multi-model mean and the grey band a range of +/- 1.0 standard deviation.

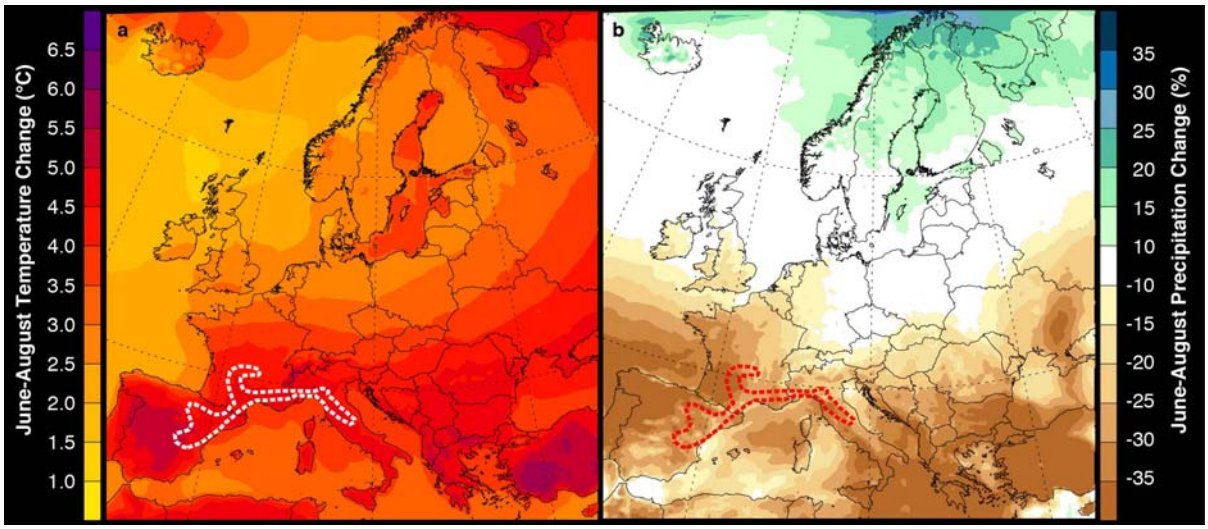

Figure S7 | Climate patterns. Projected mean **a**, June-August summer (JJA) temperature (°C) and **b**, precipitation (%) change over Europe in 2070-2099 AD with respect to the reference period 1960-1989. Shown is the ENSEMBLES multi-model mean across 12 RCMs (RCMs driven by the same GCM are averaged first to give each driving GCM equal weight) for the A1B emission scenario.